International Journal of Computing and Digital Systems
ISSN (2210-142X)
Int. J. Com. Dig. Sys. 5, No.3 (May-2016)
http://dx.doi.org/10.12785/ijcds/050305

Joint Sidelobe Suppression and PAPR Reduction Techniques in OFDM-Based Cognitive Radios, A Literature Review

Asmaa Rady[1], EL-Sayed M. El-Rabaie[2], Mona Shokair[3] and Ahmed S. Elkorany[4]

[1,2,3,4] *Dept. of Electronics and Electrical Comm., Faculty of Electronic Engineering, El-Menoufia University, Menouf, Egypt*

Received 3 Feb. 2016, Revised 1 Mar. 2016, Accepted 1 Apr. 2016, Published 1 May 2016

Abstract: Non-contiguous orthogonal frequency division multiplexing (NC-OFDM) is an efficient transmission technique in cognitive radio systems. It provides high bandwidth utilization and robustness against time dispersive channels. However, high sidelobe power and peak to average power ratio (PAPR) are the two main challenges in NC-OFDM systems. The conventional research on the literature treats these two problems individually as two independent problems, while in this paper we focus on the general performance improvement in terms of the two problems together. The general performance of all the techniques are studied and compared together through both theoretical analysis and numerical simulation. The simulation results are discussed based on the following metrics: sidelobe power, PAPR, bit error rate (BER) and system complexity. Results confirm that hybrid precoding technique is considered an optimum for all the performance measured metrics.

Keywords: NC-OFDM, PAPR, MCS, SLM, Interleaver, PTS, ACC, SSE, ACE, ACEPR, SPC, NC-SPC, BER, and SNR.

1. INTRODUCTION

NC-OFDM [1] is an ideal candidate for spectrum pooling-based wireless transmission systems which has the advantages of mitigating multi-path fading and improving the data transmission. NC-OFDM is the best modulation scheme in cognitive radio (CR) networks [2]-[4]. However, the property of multi-carriers modulation share in increasing the PAPR and sidelobe power in NC-OFDM system that cause signal distortion and degrade the frequency efficiency. The subcarriers in the vicinity of the primary users (PUs) can be deactivated and the other subcarriers are activated in order not to interfere with primary users.

Rectangular transmit pulses converts to Sinc subcarrier spectrum that has high sidelobes because of the decay of this function. The sidelobe causes large out-of-band (OOB) power levels which can potentially interfere with existing neighboring transmissions. In the other side, while the NC-OFDM symbol is a combination of sinusoids with independent amplitudes and phases, the probability of having a high instantaneous power increases, especially at large number of subcarriers. This peak to average power ratio (PAPR) [5-7] if not reduced, the power amplifier (PA) operates in the nonlinear region of the radio-frequency (RF) components and creates both spectral regrowth and self-distortion in the transmitted signal. Therefore, there is a need to significantly suppress these sidelobes and reduce the PAPR in order to make successful coexistence with adjacent systems.

The previous researches focuses on either PAPR reduction or sidelobe suppression whereas the mutual effect of these two problems are not revealed. In practical NC-OFDM systems, high PAPR and non-linearity in PA result in increasing OOB emissions which may undo the effect of using OOB emissions reduction techniques. In other hand, when the effect of PAPR and amplifier are not taken into account, sidelobe suppression techniques become ineffective for the suppressions that falls under the spectral response of the PA.

In this paper, a comparative study between the techniques that solve the two problems together is investigated. The first technique is the selective mapping with multiple choice sequence (SLM-MCS) [8]. The key idea in this technique is to generate multiple representations of the transmit signal and select a sequence with low sidelobe power and PAPR. This

E-mail address: asmaa_rady2000@yahoo.com, srabie1@yahoo.com, shokair_1999@hotmail.com, elkoranyahmed@yahoo.com

technique can reduce the OOB radiation while improving the PAPR and bit error rate (BER) for NC-OFDM signals.

The second technique is the advanced constellation expansion with peak reduction (ACEPR) [9], while partial transmit sequence (PTS) technique is used for reducing the PAPR. The ACEPR technique depends on mapping the modulation scheme to an expanded modulation scheme for a part of subcarriers. The sidelobe power for all resulting sequences is computed and the minimum sidelobe power is chosen for transmission. This technique is simpler in terms of computational complexity, achieves significant sidelobe suppression, and makes efficient use of bandwidth resources.

The third technique is similar to the first technique that based on adding interleaver to SLM-MCS technique (I-SLM-MCS) [10]. This interleaver improves the performance of PAPR, sidelobe power, and BER but increase the complexity.

The fourth technique is the hybrid precoding technique [11] which is a combination between two similar techniques, Zadoff-Chu technique [12] which reduces the PAPR and precoding technique [13] which reduces the sidelobe suppression. A different precoding matrix are multiplied in each technique therefore, it is considered a simple one. The performance of the sidelobe suppression can be adaptively adjusted with the external radio environment to improve the precoding efficiency.

The fifth technique is a MS-PTS [14] which consists of three stages. In the first and the second stages, the OFDM data vector is partitioned into contiguous blocks that are suited for PAPR reduction by PTS. While edge blocks have more impact on the OOB radiation, each edge block is further partitioned into smaller interleaved sub-blocks, and then optimized phase rotations are applied to each sub-block to suppress the spectral sidelobes. After the frequency domain techniques, the optimum phase rotation for the time domain OFDM symbol is calculated to achieve smoother transition between the consecutive symbols, which further reduces the OOB spectrum.

The sixth technique is a combination between N-Continuous technique and serial peak cancellation (NC-SPC) [15]. N-Continuous technique [16] makes derivative of high order continuous between the consecutive symbols to reduce the sidelobe power without resource redundancy. Moreover, when the derivative transformed to frequency domain by inverse discrete Fourier transform (IDFT), N-Continuous method does not cause ICI. This combined technique focuses on studying the interaction between these two kinds of techniques by mathematical model and theoretical analysis.

The seventh and final technique is the advanced cancellation carrier with signal set expansion (ACC-SSE) [17]. This technique depends on adding extra carriers in the first and last of the symbol [18], which reduce the sidelobe power and do not cause intersymbol interference, but increases PAPR and computational complexity. Therefore SSE [19] is added that depend on the fact that different sequences have different PAPR. While the important advantage in SSE technique is that there is no side information to be transmitted. This technique reduces the OOB radiation caused by high sidelobe and high PAPR.aa

The rest of the paper is organized as follows: In Section II, the system model of the original NC-OFDM technique is presented. The theory behind of each technique is presented in Section III. The performance and simulation results are discussed in Section IV. Finally, the conclusions are included in Section V, followed by the references.

2. SYSTEM MODEL

CR system employs NC-OFDM as the main modulation scheme, because this system is familiar with the radio scenario and the channel state information (CSI).The spectrum sensing is the basic stages in cognitive radio networks, which detects the occupancy of the spectrum. This sensing deactivates the subcarriers that are located in PU band and activates the other unoccupied spectrum to be free for using by any secondary user. After the spectrum sensing, the interference between the PUs and secondary users (SUs) is minimized.

A general schematic of NC-OFDM system shown in Fig.1 considers K subcarriers while the input serial bits are mapped to Quadrature Phase Shift Keying (QPSK) mapping modulation and then serial to parallel conversion giving K parallel constellation points which represent the data. The IDFT which converts the data from frequency domain to time domain, is applied to these streams modulating them to different subcarrier center frequencies. The parallel to serial conversion converts the obtained sequence to serial stream then cyclic prefix is inserted at the beginning of each OFDM symbol with guard interval exceeding delay spread of the multipath channel to reduce the effect of intersymbol interference (ISI). This sequence is converted to analog signal $x(\mathrm{t})$ while this signal is up converted to the desired frequency, is amplified by power amplifier, and finally is transmitted.

Define $\mathrm{X} = [X_0, X_1, \ldots\ldots, X_{K-1}]^T$ is an input symbol in frequency domain after QPSK mapping, K is the number of subcarriers, X_k is the complex data of the kth subcarrier, and [.]T denotes transpose. The OFDM sequence $\mathrm{x} = [x_0, x_1, \ldots\ldots, x_{K-1}]$ is the IDFT of X. The complex envelope of the baseband NC-OFDM

signal is the output of D/A converter which is defined over the time interval $t \in [0, T_s]$ as,

$$x(t) = \frac{1}{K}\sum_{k=0}^{K-1} X_k\, e^{j2\pi kt/T_s} \qquad (1)$$

where, T_s is OFDM symbol duration. The symbol over the kth deactivated subcarrier is $X_k = 0$. The discrete K samples of NC-OFDM signal are computed by IDFT which is referred as,

$$x_n = \frac{1}{K}\sum_{k=0}^{K-1} X_k\, e^{\frac{j2\pi kn}{K}} \qquad n = 0, \ldots, K-1 \qquad (2)$$

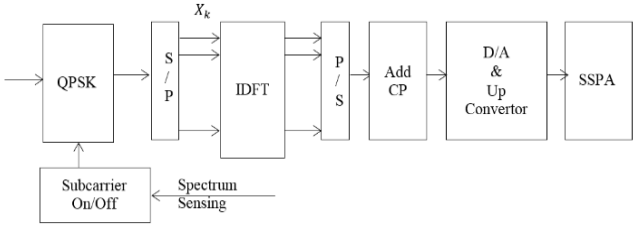

Figure 1: Block diagram of the original NC-OFDM system.

The PAPR is defined as the ratio between maximum instantaneous power to the average power, and is given by,

$$\text{PAPR}[x(t)] = \frac{\max_{0\le t<T_0} |x(t)|^2}{E[|x(t)|^2]} \qquad (3)$$

3. JOINT SIDELOBE SUPPRESSION AND PAPR REDUCTION TECHNIQUES

A- SLM with MCS

The main idea of this technique is to map each transmission sequence into specific sets of sequences that can be exploited by the original MCS [20] and SLM [21] techniques which reduce the sidelobe power and PAPR, respectively. The MCS and SLM are applied after S/P converter as shown in Fig. 2. The data is multiplied with multiple phase and is fed to MCS to obtain the sequences $X_k^{r(c)}, c = 1, \ldots\ldots, D$. The NC-OFDM discrete time symbols $x_n^{r(c)}, c = 1, \ldots\ldots, D$, are then obtained via the IDFT operation. Finally PAPR are computed for D sequences and the lowest PAPR sequence $x_n^{c'}$ is selected.

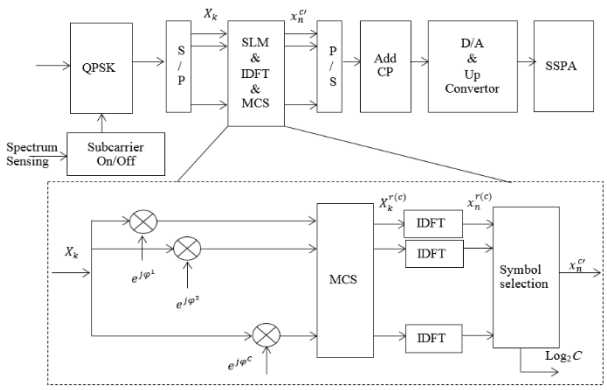

Figure 2: Block diagram of the NC-OFDM including SLM and MCS techniques [8].

From the fact that changing the phase shifts of the data leads to a significant effect on PAPR and sidelobe power of NC-OFDM signal. Therefore in SLM, C alternative input symbol sequences can be generated from the same input symbol sequence X and the sequence with minimum PAPR is used for transmission. These C sequences $X^c = [X_0^c, \ldots\ldots, X_{K-1}^c]$ are generated by multiplying the input sequence X with C independent phase sequences as expression

$$X_k^c = X_k e^{j\varphi_k^c}, \qquad 1 < c < C \qquad (4)$$

where φ_k^c is a uniformly distributed random variable over $[0, 2\pi]$.

MCS technique is similar to SLM technique which also generates an alternative sequence from the original NC-OFDM sequence and finally the sequence with the lowest sidelobe power is chosen for transmission. Here a rectangular pulse-shape is applied for the kth subcarrier of the transmitted signal. Therefore the spectrum of an individual subcarrier equals a si-function. The average sidelobe power in adjacent PU frequency band is expressed as [22],

$$\Lambda_c = \frac{1}{N}\sum_{n=1}^{N}\left|\sum_{k=0}^{K-1} X_k^c \frac{\sin(\pi(F_n' - F_k))}{\pi(F_n' - F_k)}\right|^2 \qquad (5)$$

where, $F_n', n = 1, \ldots, N$ is the normalized frequency samples within the adjacent PU frequency bands which is normalized to the subcarrier spacing and $F_k, k = 0, \ldots, K-1,$, is the normalized center frequency of the kth subcarrier.

Then those average sidelobe power Λ_c must be ranked giving $\Lambda_{r(1)} \le \ldots \le \Lambda_{r(C)}$. $r(C)$ gives the rank, and selects the D ones with lowest sidelobe power instead of selecting the minimum sidelobe power. D is the number of sequences considered for computing the PAPR reduction $D < C$. The sequences that is related to

those D lowest sidelobe power $X_k^{r(c)}, c = 1, \ldots, D$, according to $\Lambda_{r(1)}^m \ldots \Lambda_{r(D)}^m$ are chosen. Then taking the IDFT of $X_k^{r(c)}$ gives,

$$x_n^{r(c)} = IDFT\{X_k^{r(c)}\} \qquad , c = 1, \ldots, D \tag{6}$$

Finally, the PAPR for D alternative OFDM sequence can be computed and the lowest one $x_n^{c'}$ can be chosen for transmission, as shown in the following equation,

$$c' = \arg \min_{1<c\leq D} \text{PAPR}\left[x_n^{r(c)}\right] \tag{7}$$

The computational complexity increases when the number of alternative sequence increases while PAPR and sidelobe power is decreased. This occurs due to the increase of the number of IDFT required for generating C alternative OFDM sequences. A number of C phase sequences must be known to both the transmitter and receiver and $\log_2 C$ bits of explicit side information per OFDM symbol must be transmitted.

B- Advanced Constellation Expansion with Peak Reduction

The basic idea is to combine between two techniques, advanced constellation expansion ACE and partial transmit sequence PTS that reduce the sidelobe power and PAPR, respectively. In the CE technique [23], the symbol of a modulation scheme (QPSK) consisting of 4 constellation points is mapped to a modulation scheme (8-PSK) consisting of 8 constellation points. In the expanded constellation, two points are associated with each point in the original constellation. The idea of the CE technique is to calculate the sidelobe power for different combinations which gives different values and choose the sequence with the minimum sidelobe power for transmission.

The frequency domain representation for the kth OFDM subcarrier as in [24] is given by:

$$S_k(F) = \frac{T_s}{\sqrt{K}} e^{-j\pi(F-F_k)\alpha_{cp}} \frac{\sin(\pi(F-F_k)\alpha_{cp})}{\pi(F-F_k)\alpha_{cp}} \tag{8}$$

where T_s is the symbol period including the cyclic prefix period T_{cp} (i.e. $T_s = T_0 + T_{cp}$). f represents the frequency and F is normalized frequency shifted to the center frequency f_c of the OFDM system which is normalized to the subcarrier spacing $(1/T_0)$, (i.e. $F = (f - f_c)T_0$). Also, $F_k = (f_k - f_c)T_0$ is the normalized center frequency of the kth subcarrier with $f_k = k/T_0$. The effect of the cyclic prefix is $\alpha_{cp} = 1 + T_{cp}/T_0$. The sidelobe emission for an OFDM symbol with K subcarriers can be calculated using the following equation:

$$e(F) = \sum_{k=1}^{K} X_k S_k(F) \tag{9}$$

Where X_k is the input data symbol, modulating the kth subcarrier. The basic idea in ACE is that the sidelobe power is decreased when the sidelobes of different subcarriers add up destructively. The ACE technique combines this idea with the CE idea therefore, instead of selecting the points from a larger constellation on a random fashion, points are chosen which reduces the sidelobe efficiently. In ACE, constellation expansion is done only at the border of OFDM symbols while the remaining subcarriers are kept unexpanded, hence the complexity is reduced.

The ACE technique divides OFDM symbols into three groups as shown in Fig. 3. The expansion is done for the first and the last L subcarriers only, while the remaining $K - 2L$ subcarriers are kept unexpanded. For the kth subcarrier, we define $S_{k,l}$ and $S_{k,r}$ as the frequency domain representations in the sidelobe range to the left, and to the right of OFDM spectrum, respectively. Let $X_{k,1}, X_{k,2}$ are the points in the expanded constellation set which are related to X_k in the original constellation set. ACE technique is explained in the following mapping while expanding the first L subcarriers is considered and is shown in the following steps [9]:

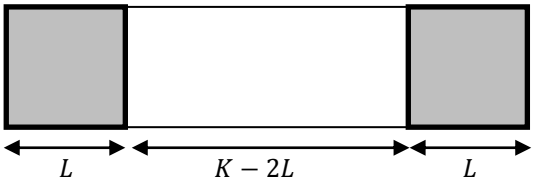

Figure 3: OFDM symbol structure in the ACE technique [9].

Calculate the sidelobe emission of the left OFDM spectrum due to the unexpanded data symbols using:

$$e_{0,l}(F) = \sum_{k=L+1}^{K-L} X_k S_{\boldsymbol{k,l}}(F) \tag{10}$$

Set $i = 1$.

For the ith subcarrier ($i \leq L$), the sidelobe emission due to $X_{i,1}, X_{i,2}$ which are related to X_i, is calculated as:

$$\tilde{e}_{\boldsymbol{i}1}(F) = e_{(i-1),l}(F) + X_{i1} S_{i,l}(F) \tag{11}$$

$$\tilde{e}_{\boldsymbol{i}2}(F) = e_{(i-1),l}(F) + X_{i2} S_{i,l}(F) \tag{12}$$

The sidelobe power of (11) and (12) are calculated using the following equation:

$$P_{i1} = \int \|\tilde{e}_{i1}(F)\|^2 \, dF \tag{13}$$

$$P_{i2} = \int \|\tilde{e}_{i2}(F)\|^2 \, dF \tag{14}$$

If $P_{i1} < P_{i2}$, then X_i is mapped to X_{i1} , and

$$e_{i,l}(F) = \tilde{e}_{i1}(F) \tag{15}$$

Otherwise X_i is mapped to X_{i2} and

$$e_{i,l}(F) = \tilde{e}_{i2}(F) \quad (16)$$

Increment i

If $(i \leq L)$, go to step 3.

Note that the same procedure is applied for the last L subcarriers which are used to suppress the sidelobe emissions to the right of OFDM spectrum. Therefore, a significant OOB emissions reduction can be achieved on both sides of OFDM spectrum.

While φ represents the phase difference between two points in the expanded constellation that are related to the same point in the original constellation therefore, φ can be $\pi/4$, $\pi/2$, $3\pi/4$, or π. The ACE technique can achieve better sidelobe suppression when $\varphi = \pi$ because at each assignment there are two out-of-phase contributions in the sidelobe power and only one of them results in lowering the sidelobe power.

Applying the ACE technique on NC-OFDM system leads to increase the PAPR depends on φ and L. To overcome this problem, PTS [25] technique is combined with the ACE technique. This can be done by mapping the original data sequence that represents the unexpanded subcarriers into another transmission sequence using PTS which reduces the PAPR. PTS can be modified to work properly with the ACE technique as follows:

(1) Divide $K - 2L$ subcarriers (unexpanded subcarriers) into N_b blocks in the frequency domain. Each block consists of $(K - 2L)/N_b$ subcarriers. Then each of these blocks are multiplied with Q different PTS vectors.

(2) Apply the ACE technique to expand the $2L$ subcarriers for each of the Q different sequences. Then unity gain is applied to the $2L$ subcarriers.

(3) Take Q IDFTs to find the time-domain symbols and compute the PAPR for each one and finally the sequence with minimum peak amplitude is chosen for transmission.

For example, consider the system shown in Fig. 4 ($L = K/8,\ N_b = 3$). The first and the last L subcarriers have unit gain (zero phase shift), while the remaining $3K/4$ subcarriers are divided into three blocks each of length $K/4$. Each of these blocks is multiplied by different phase shift resulting in $Q = 4$ different frequency domain sequences. Then, the ACE technique is applied for each of these different sequences. After taking the IDFT of each sequence (with the corresponding ACE subcarriers), the PAPR is computed for each time-domain symbol and finally the lowest one is chosen for transmission.

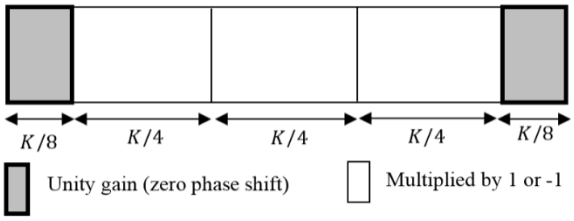

Figure 4: OFDM symbol structure in the ACE with PTS techniques [9].

C- Interleaver with SLM and MCS

This technique is similar to the previous technique while it depends on SLM and MCS as shown in Fig. 5, to reduce the PAPR and sidelobe together. The difference in this technique is adding interleaver to give more reduction to PAPR and sidelobe.

M interleavers are added to the transmitter, which these interleavers produce M permuted sequences of the input data in pseudorandom order. The resulting sequences are given by,

$$X_k^m = X_{\Pi_k^m} \quad (17)$$

where, $k = 1, \ldots, K-1,\ m = 1, \ldots, M,\ \Pi_k^m \in \{0, \ldots, K-1\}$ are permutation indices stored at the transmitter and the receiver. The number of different alternative sequence $\mathrm{X}^m = (X_0^m, \ldots, X_{K-1}^m)$ with the interleaving approach decreases when the original sequence X contains repetitive data symbols such as $\mathrm{X} = (1, 1, 1, \ldots, 1)^T$. All those sequences fed to MCS and SLM which finally compute the sidelobe power and PAPR for them and the minimum sidelobe power and PAPR sequence is chosen for transmission.

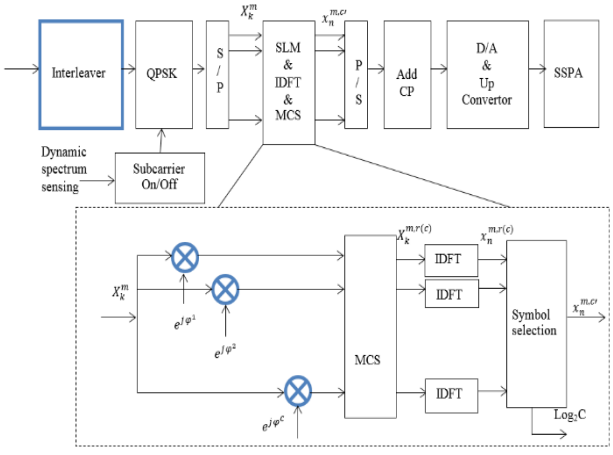

Figure 5: Block diagram of a NC-OFDM transmitter with the Interleaver, SLM, and MCS techniques [10].

SLM takes sequence by sequence from the interleaver after modulation and each of m sequence is multiplied by random phase $e^{j\varphi_k^c}$ as follows:

$$X_k^{m,c} = X_k^m e^{j\varphi_k^c},\ \ \varphi_k^c \in [0,2\pi],$$
$$c = 1, \dots., C,\ \ m = 1, \dots M \qquad (18)$$

Then MCS computes the average sidelobe power for each of the sequences over N samples as this equation:

$$\Lambda_c^m = \frac{1}{N}\sum_{n=1}^{N}\left|\sum_{k=0}^{K-1} X_k^{m,c}\frac{\sin(\pi(F_n' - F_k))}{\pi(F_n' - F_k)}\right|^2 \qquad (19)$$

As the previous technique the average sidelobe power is ranked giving $\Lambda_{r(1)}^m \leq \dots \leq \Lambda_{r(C)}^m$. $r(C)$ gives the rank, and selects the D ones with lowest sidelobe power and OOB while $D < C$. The sequences that corresponding to those D lowest sidelobe power $X_k^{m,r(c)}$, $c = 1, \dots., D$, related to $\Lambda_{r(C)}^m \dots \Lambda_{r(D)}^m$ are chosen. Then $x_n^{m,r(c)}$ are computed by,

$$x_n^{m,r(c)} = IDFT\{X_k^{m,r(c)}\} \qquad (20)$$

Finally, the PAPR is computed and the lowest PAPR from the D sequences that corresponding to only m sequences is given by,

$$c_m' = \arg\min_{1<c\leq D} \text{PAPR}\left[x_n^{m,r(c)}\right] \qquad (21)$$

and also find the lowest PAPR from the m permuted frames by,

$$c' = \arg\min_{1<m\leq M} c_m' \qquad (22)$$

A number of C phase sequences and M permuted frames with their corresponding indexes c, m must be known to both the transmitter and the receiver. Therefore, there are $\log_2 M$ and $\log_2 C$ bits of explicit side information per OFDM symbol. With increasing of C phase sequences and M permuted frames, this technique will be more complex.

D- Hybrid Precoding Technique

Two precoding stages are added before IDFT as shown in Fig. 6, the first stage is Zadoff-Chu transform (ZCT) which transform the original vector to a new vector with low PAPR and the second precoding stage is applied to produce another vector with low sidelobe power.

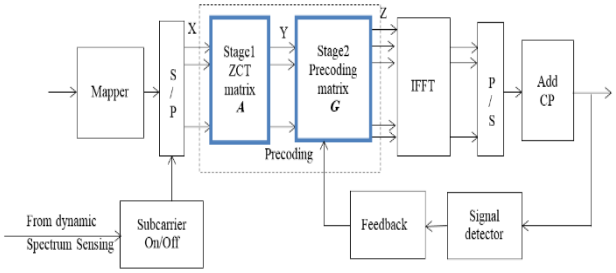

Figure 6: Block diagram of an NC-OFDM with hybrid precoding technique [11].

1) Zadoff-Chu sequence for PAPR reduction:

Zadoff-Chu sequences are class of poly phase sequences that have optimum correlation properties. They have an ideal periodic autocorrelation and constant magnitude. These sequences of length $\mathcal{L}$ is defined according to [13] as:

$$a(\ell) = \begin{cases} e^{\frac{j2\pi r}{\mathcal{L}}\left(\frac{\ell^2}{2} + q\ell\right)} & \text{for } \mathcal{L} \text{ even} \\ e^{\frac{j2\pi r}{\mathcal{L}}\left(\frac{\ell(\ell+1)}{2} + q\ell\right)} & \text{for } \mathcal{L} \text{ odd} \end{cases} \qquad (23)$$

where $\ell = 0, 1, \dots\dots, \mathcal{L}-1$, r is any integer relatively prime to $\mathcal{L}$, and q is any integer number.

The kernel of the ZCT acts as a column-wise ZCT matrix $\boldsymbol{A}$ of dimension $\mathcal{L} = K \times K$ which is obtained by reshaping the ZC sequence with $\ell = r + kK$ as this equation:

$$\boldsymbol{A} = \begin{bmatrix} a_{00} & a_{01} & \cdots & a_{0(K-1)} \\ a_{10} & a_{11} & \cdots & a_{1(K-1)} \\ \vdots & \vdots & a_{rk} & \vdots \\ a_{(K-1)0} & a_{(K-1)1} & \cdots & a_{(K-1)(K-1)} \end{bmatrix} \qquad (24)$$

Here k is the column variable and r is the row variable. In other words, the $\mathcal{L} = K^2$ points long ZC sequence fill the kernel of the matrix. This matrix is multiplied by the original vector X as given by:

$$\text{Y} = \boldsymbol{A}\,\text{X} \qquad (25)$$

where $\text{Y} = [y_0, y_1, \dots., y_r, ., y_{K-1}]^T$ is the output vector from ZCT with the same length K. The rth symbol y_r can be written as:

$$y_r = \sum_{k=0}^{K-1} a_{r,k} X_k, \qquad r = 0, 1, \dots\dots, K \qquad (26)$$

where $a_{r,k}$ means rth row and kth column of the ZCT matrix. $a_{r,k}$ is computed from eq. (23) by using column wise reshaping $\ell = r + kK$ and putting $r = 1$ and $q = 0$. Therefore, the resulting vector Y has low PAPR but it still has high sidelobe power.

2) Precoding technique for reducing sidelobe power:

This is the second stage which is applied to the vector Y with low PAPR to reduce the sidelobe power and converts this vector to resulting vector $\mathrm{Z} = [z_0, z_1, .., z_m .., z_{\mathcal{M}-1}]^T$.

$$\mathrm{Z} = \boldsymbol{G}\mathrm{Y} \tag{27}$$

where $\boldsymbol{G}$ is $\mathcal{M} \times K$ complex valued orthogonal precoding matrix with $\mathcal{M} \geq K$, i.e. $\boldsymbol{G}^H\boldsymbol{G} = \boldsymbol{I}$. The subscript [.]H denotes conjugate transposition and $\boldsymbol{I}$ is identity matrix. $R = \mathcal{M} - K$ is defined as precoding redundancy and also $\rho = K/\mathcal{M}$ is precoding efficiency.

The resulting vector is modulated onto $\mathcal{M}$ subcarrier by IDFT, then CP with length η is inserted to the output of IDFT. The OFDM symbol $S = [s_0, \ldots, s_j .., s_{\mathcal{J}-1}]^T$, where $\mathcal{J} = \mathcal{M} + \eta$ is generated. Where s_j is the jth component of S and is defined as,

$$s_j = \frac{1}{K}\sum_{m=0}^{\mathcal{M}-1} z_m \, e^{j2\pi m(j-\eta)/\mathcal{M}} \tag{28}$$

The frequency domain representation of OFDM symbols is obtained by the Fourier transform of S and is given by:

$$S'(f) = \sum_{j=0}^{\mathcal{J}-1} s_j \, e^{-j2\pi f j T_0} \tag{29}$$

This equation is written in the vector form to be easy used in this form:

$$S'(f) = \frac{1}{K} E\, \boldsymbol{F}^H \boldsymbol{D}\, \boldsymbol{G}\, Y = \frac{1}{K} E\, \boldsymbol{F}^H \boldsymbol{D}\, \boldsymbol{G}\, \boldsymbol{A}\, X \tag{30}$$

where $E = (1, e^{-j2\pi f T_s}, e^{-j2\pi 2 f T_s}, \ldots\ldots\ldots\ldots, e^{-j2\pi(\mathcal{J}-1) f T_s})$ is $1 \times \mathcal{J}$ vector, F is an $\mathcal{M} \times \mathcal{J}$ Fourier matrix with (m, j)th entry of $e^{j2\pi m j/\mathcal{M}}$, and $\boldsymbol{D}$ is diagonal matrix which denotes CP matrix $\boldsymbol{D} = \mathrm{diag}\,(1, e^{-j2\pi\eta/\mathcal{M}}, \ldots\ldots\ldots\ldots, e^{-j2\pi(\mathcal{M}-1)\eta/\mathcal{M}})$. Assume the frequency region $B_{\mathcal{C}} = [f_D, f_U]$ assigned to PU is detected. The main goal is to exploit the spectrum with less interference with PU and high efficiency. The basic factors that determine the interference with PU is the matrix E and the jth component of $e^{-j2\pi f j T_s}$ in the frequency region $f \in [f_D, f_U]$. The interference spectral leakage of the vector S in $B_{\mathcal{C}}$ can be evaluated by two times sampling of the frequency f in the matrix E in $B_{\mathcal{C}}$ which is collected in $\{f_0, f_1, \ldots\ldots, f_{\mathcal{C}-1}\} \in B_{\mathcal{C}}$. The Fourier transform of each OFDM symbol at these frequencies are forced to be zero in order to reduce the interference with PU.

$$S'(f_c) = 0 \qquad c = 0, 1, \ldots\ldots, \mathcal{C} - 1 \tag{31}$$

The OFDM spectrum cancels each other with the help of the precoding matrix $\boldsymbol{G}$ by introducing the correlation to subcarrier if well designed. Equations (30) and (31) results:

$$\gamma\, \boldsymbol{G}\, \boldsymbol{A}\, X = 0, \qquad \gamma = E\, \boldsymbol{F}^H \boldsymbol{D} \tag{32}$$

The average power spectrum of OFDM symbol will also equal zero at these frequency samples and their vicinity. Therefore, the power spectrum of the precoded OFDM symbol and uncoded symbol should be the same. Due to the orthogonality of the precoding matrix $\boldsymbol{G}$, it should satisfy

$$\boldsymbol{G}^H\, \boldsymbol{G} = \boldsymbol{I}_K \tag{33}$$

This means that each precoded OFDM symbol has the same amplitude as that before precoded. Therefore the PAPR does not change before and after the precoding process and it still be in the low range.

The basic idea in this technique is using singular value decomposition (SVD) to solve the problem of the last two equations by decomposing γ into:

$$\gamma = \boldsymbol{U}\, \boldsymbol{\Sigma} \boldsymbol{V}^H \tag{34}$$

where $\boldsymbol{U}, \boldsymbol{V}$ are two unitary matrices with size $\mathcal{C} \times \mathcal{C}$ and $\mathcal{M} \times \mathcal{M}$, respectively. This unitary means that $\boldsymbol{U}^H \boldsymbol{U} = \boldsymbol{I}_{\mathcal{C}}$ and $\boldsymbol{V}^H \boldsymbol{V} = \boldsymbol{I}_{\mathcal{M}}$. Define $\boldsymbol{\Sigma}$ is $\mathcal{C} \times \mathcal{M}$ diagonal matrix with singular values filled in its diagonal in non-increasing order. Therefore, the optimal precoding matrix can be considered as orthogonal basis of null space of γ

$$\boldsymbol{G} = \boldsymbol{V}_G \boldsymbol{Q} \tag{35}$$

where $\boldsymbol{V}_G$ is $\mathcal{M} \times K$ submatrix of $\boldsymbol{V}$ while $\boldsymbol{V}_1$ is consist of the last K columns in $\boldsymbol{V}$, and $\boldsymbol{Q}$ is an arbitrary $K \times K$ unitary matrix. The submatrix $\boldsymbol{V}_G$ is orthogonal to satisfy the constrain in Eq. (33). The sidelobe power leakage after precoding is given by:

$$W_G = \delta \sum_{i=R}^{\mathcal{M}-1} \boldsymbol{\Sigma}_{i,i} \tag{36}$$

where δ is constant coefficient. The sidelobe power leakage is associated with singular value of $\boldsymbol{A}$. More interference is suppressed with discarding more singular values of matrix $\boldsymbol{A}$ by precoding matrix $\boldsymbol{G}$. The sidelobe power decreases with increasing the precoding redundancy R. The first biggest singular values R can be discarded adaptively due to the feedback from channel statues.

The PAPR is the ratio between maximum instantaneous power to the mean power, and is defined as:

$$\text{PAPR} = \frac{\max|s_j|^2}{E\left[|s_j|^2\right]} \quad (37)$$

E- Multi-Stages of Partial Transmit Sequence

It is consists of three-stages for jointly reducing the OOB radiation and PAPR as shown in Fig.7. The key idea in this technique is a phase rotation of the blocks and subblocks of the data vector $\mathrm{X}^{(i)} = [(X_0^{(i)}, X_1^{(i)}, \ldots\ldots, X_{K-1}^{(i)}]^T$ in the ith OFDM symbol. There are two level of partitioning the data vector, the first level is splitting $\mathrm{X}^{(i)}$ into V distinct and consecutive blocks $\mathrm{X}_v^{(i)}$, $v = 0,1,\ldots,V$ where each block is independently phase-rotated for minimizing instantaneous peak power. This first level partition is formulated as [14]:

$$[\mathrm{X}_v^{(i)}]_k = \begin{cases} [\mathrm{X}^{(i)}]_k & (v-1)\frac{K}{V} \le k \le v\frac{K}{V} \\ 0 & elsewise \end{cases} \quad (38)$$

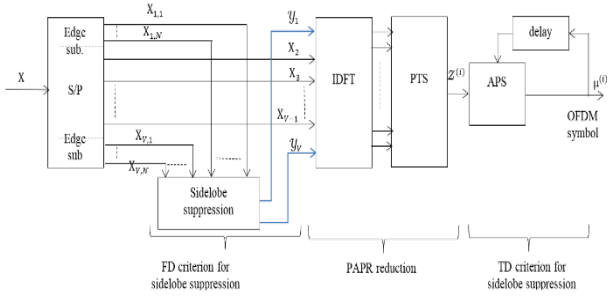

Figure 7. Block diagram of the three-stage technique [14].

where $[\mathrm{X}]_k$ denotes the kth element of the data vector X. The second level of partitioning is splitting the two blocks that are located in the band edges (first and last blocks) into $\mathcal{N}$ subblocks $\mathrm{X}_{v,n}^{(i)}$, $v = 1, V$ *and* $n = 1, 2, \ldots\ldots, \mathcal{N}$. These subblocks are interleaved by taking the first elements from each subblock together then the second elements and then the third elements and so on to form $\mathcal{N}$ interleaved subblocks that is given by:

$$[\mathrm{X}_{v,n}^{(i)}]_k = \begin{cases} [\mathrm{X}_v^{(i)}]_k & k = n + q\mathcal{N}, q = 0, \ldots. , \frac{K}{V\mathcal{N}} - 1 \\ 0 & elsewise \end{cases} \quad (39)$$

1) Stage 1: sidelobe suppression with frequency domain criterion

The edge subcarriers have more effect on the OOB radiation than the inner subcarriers [26], because each subcarrier's spectrum decays monotonically. In this stage only the first and last blocks of subcarriers that lay in the edge are taken into account for sidelobe suppression. Each block from these two blocks are spilt into $\mathcal{N}$ interleaved subblock as Eq. (39) in order to reduce the sidelobe power with applying suitable phase shifts that has the most effect on the signal spectrum and achieves more degree of freedom. The first and last blocks are modified by this equation:

$$[\mathcal{Y}_v^{(i)}]_k = \sum_{n=1}^{\mathcal{N}} \lambda_{v,n}^{(i)} \mathrm{X}_{v,n}^{(i)}, \qquad v = 1, V \quad (40)$$

where $\lambda_{v,n}^{(i)}$ is a complex number with unity amplitude which shifts the phase of the nth subblock of the vth block in the ith OFDM symbol. The sidelobe power of the combined interleaved subblocks which should be minimized is given by:

$$P_I = \|\mathfrak{X}_v \mathcal{Y}_v\|^2 = \left\| \sum_{n=1}^{\mathcal{N}} \mathfrak{X}_v \lambda_{v,n} \mathrm{X}_{v,n} \right\|^2, \quad (41)$$

where $v = 1, V$, $\mathfrak{X}_v$ is an $\mathcal{P} \times K$ interference matrix which gives the contribution of each subcarrier at $\mathcal{P}$ frequency locations on the sidelobe spectrum. The normalized frequency of the spectrum is F_1 and F_V for the lower and upper sidelobe, respectively. The interference matrix is given by:

$$[\mathfrak{X}_v]_{p,k} = \frac{\sin(\pi \frac{\eta+K}{K}([F_v]_p - k))}{\pi \frac{\eta+K}{K}([F_v]_p - k)},$$

$$k = 1, \ldots, K \quad p = 1, \ldots, \mathcal{P} \quad v = 1, V \quad (42)$$

where η is the length of cyclic prefix. The sidelobe power that needs to be reduced is written in the matrix form as this equation:

$$P_I = \|\mathfrak{X}_v \boldsymbol{\chi}_v \lambda_v\|^2 = \lambda_v^H \boldsymbol{\chi}_v^H \ \mathfrak{X}_v^H \ \mathfrak{X}_v \ \boldsymbol{\chi}_v \lambda_v \quad (43)$$

where $\lambda_v = [\lambda_{v,1}, \lambda_{v,2}, \ldots\ldots, \lambda_{v,\mathcal{N}}]^T$ and $\boldsymbol{\chi}_v = [\mathrm{X}_{v,1}, \mathrm{X}_{v,2}, \ldots\ldots, \mathrm{X}_{v,\mathcal{N}}]$. While $\boldsymbol{\mathcal{A}}_v = \boldsymbol{\chi}_v^H \mathfrak{X}_v^H \mathfrak{X}_v \boldsymbol{\chi}_v$, the aim is to minimize $P_I = \lambda_v^H \boldsymbol{\mathcal{A}}_v \lambda_v$ by optimization problem subject to

$$|[\lambda_v]_n|^2 = 1, \quad n = 1, \ldots\ldots, \mathcal{N} \quad (44)$$

This optimization problem falls under the family of quadratically constraint quadratic programs (QCQP) which have efficient solutions to solve this problem, e.g., semidefinite relaxation [27]. Selecting independent phase rotation for each subcarrier, minimizes sidelobe power but increases the complexity and the number of phases to be sent to the receiver.

After determining the phase vectors and combining the subblocks for the first and last blocks as in (40), the data blocks which two of them are the output of the first stage and the remaining are the input data are converted to time-domain blocks with IDFT. Therefore, the output of IDFT becomes V time domain vectors which also the input of the PAPR reduction stage that can be written as

$$\mathcal{Y}_v = \begin{cases} \mathbf{F}^H \mathcal{Y}_v & v = 1, V \\ \mathbf{F}^H \mathrm{X}_v & v = 2, 3, \ldots\ldots, V-1 \end{cases} \quad (45)$$

where $\mathbf{F}^H$ is $(K+\eta) \times K$, IDFT matrix that generate CP-OFDM symbol.

2) Stage 2: PAPR reduction with PTS

The main idea of PTS [28] technique is based on shifting the phases of the partitions of the OFDM data vector in order to reduce the PAPR of the resulting vector. The resulting vector is given by

$$\mathcal{Z} = \sum_{v=1}^{V} \beta_v \mathcal{Y}_v \qquad v = 1, \ldots, V \quad (46)$$

where β_v is the phase rotation that performed in vth block in order to minimize the PAPR as this equation

$$\text{minimize} \max_{0 \le \hbar < K} \left(K \frac{|[\mathcal{Z}]_\hbar|^2}{\mathcal{Z}^H \mathcal{Z}} \right) \quad (47)$$

Therefore, a simple quantized-PTS algorithm is adopted in which finite set of quantized phases is considered [28], i.e., $\beta_v \in \left\{1, e^{j2\pi\frac{1}{\mathcal{R}}}, \ldots\ldots, e^{j2\pi\frac{\mathcal{R}-1}{\mathcal{R}}}\right\}$. In the PTS stage, the phase rotations of the first and last blocks ($\mathcal{Y}_1\beta_1$ and $\mathcal{Y}_V\beta_V$) does not affect the performance of sidelobe suppression because the power level of the combined interleaved subblocks is maintained after the corresponding phase shifts.

3) Stage 3: sidelobe suppression with time domain criterion

While the phase rotation does not affect the sidelobe suppression performance therefore, applying a constant phase shift to the OFDM symbol does not affect the previous two stages. This additional degree of freedom is considered to improve the transition between two consecutive OFDM symbols and further improve the spectral sidelobe. As shown in Fig.8, the symbol boundary that have sharp transitions is phase-smoothed after shifting the phase of the current symbol adaptively.

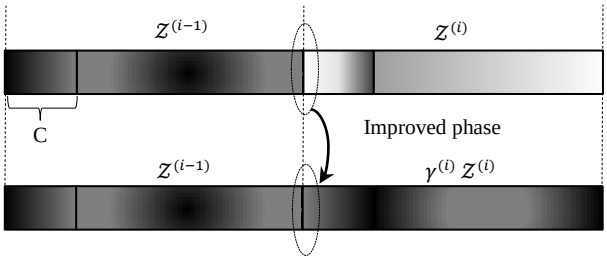

Figure 8. Phase rotation of the OFDM symbol that make the transition smoother [14].

By restoring the symbol index, the phase shift $\Lambda^{(i)}$ is applied on the output of the second stage $\mathcal{Z}^{(i)}$ while the output , $\mu^{(i)} = \Lambda^{(i)}\mathcal{Z}^{(i)}$ becomes the ith OFDM symbol to be transmitted. While the previous symbol is $\mathcal{Z}^{(i-1)}$, the phase shift that used to provide the best phase transition between the end of the $(i-1)$th symbol and the start of the ith symbol, reduces the sidelobe power of the concatenated time domain vector which is defined as

$$P_I^{(i)} = \left\| \boldsymbol{\mathcal{F}}_{\mathcal{P},\zeta} \begin{bmatrix} \mathcal{Z}^{(i-1)} \\ \Lambda^{(i)}\mathcal{Z}^{(i)} \end{bmatrix} \right\|^2 \quad (48)$$

where $\boldsymbol{\mathcal{F}}_{\mathcal{P},\zeta}$ is an $\mathcal{P} \times \zeta$ interference matrix which projects the ζ-length time domain vector to the $\mathcal{P}$ frequency locations in the OOB while $\zeta = 2(K+\eta)$. This matrix is subset of the $\zeta \times \zeta$ discrete Fourier transform (DFT) matrix that contains only the rows corresponding to the sidelobe frequencies whose power is to be minimized. When $\Lambda^{(i)} = e^{j\theta_i}$ and the linearity of matrix multiplication is used, this equation can be rewrite as

$$P_I^{(i)} = \left\| \mathbf{a} + e^{j\theta_i}\mathbf{b} \right\|^2 \quad (49)$$

where $\mathbf{a} = \boldsymbol{\mathcal{F}}_{\mathcal{P},\zeta} \begin{bmatrix} \mathcal{Z}^{(i-1)} \\ [0]_{(K+\eta)\times 1} \end{bmatrix}$ and $\mathbf{b} = \boldsymbol{\mathcal{F}}_{\mathcal{P},\zeta} \begin{bmatrix} [0]_{(K+\eta)\times 1} \\ \mathcal{Z}^{(i)} \end{bmatrix}$. The optimum angle that minimizes the sidelobe power $P_I^{(i)}$ is the angle which minimize the Eq. (49). Therefore, this angle is the solution of this equation:

$$\frac{\partial}{\partial \theta_i} \left\| \mathbf{a} + e^{j\theta_i}\mathbf{b} \right\|^2 = 0 \quad (50)$$

which yield

$$e^{j2\theta_i} = \frac{\mathbf{b}^H \mathbf{a}}{\mathbf{a}^H \mathbf{b}} \quad (51)$$

The phase angle in (49) becomes the angle of the inner product of the sidelobe vectors achieved from the previous and the current symbols, i.e., $\theta_i = \angle\langle \mathbf{b}, \mathbf{a} \rangle$.

F. Joint N-Continuous and SPC

In this technique two techniques are used to reduce both sidelobe power and PAPR which combines N-continuous and serial peak cancellation (SPC) while two blocks are added before the IDFT block the first block is N-continuous then SPC as Fig. 9. The key idea in the N-continuous technique which used for reducing the sidelobe power depends on the fact that consecutive symbols with strong continuity have low sidelobe, while the continuity is enhanced with the continuity of derivative of higher order. Therefore, in order to improve the continuity between any two symbols, N-Continuous renders the transmitted signal $x(t)$ to let its first N' derivatives satisfy [29]

$$\frac{d^n}{dt^n}x_i(t)\Big|_{t=-T_{cp}} = \frac{d^n}{dt^n}x_{i-1}(t)\Big|_{t=T_s} \quad (52)$$

where $x_i(t)$ is the ith baseband NC-OFDM symbol. Then the updated signal vector after N-continuous $\overline{\mathbf{x}}_i$ is the sum of original signal vector $\mathbf{x}_i$ and a smallest suppression vector $\mathbf{w}_i$, while $\overline{\mathbf{x}}_i = \mathbf{x}_i + \mathbf{w}_i$. After solving this matrix equation, it introduces artificial additional distortion $\mathbf{w}_i$ to signal to smooth consecutive symbols.

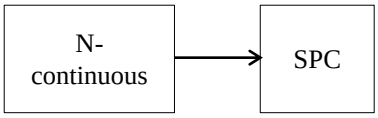

Figure 9. The model of the combined methods of N-continuous and SPC [15].

The spectrum of NC-OFDM can be divided into multiple non-consecutive subbands, the sidelobes of each subband can be processed by individual N-Continuous technique parallelly. While J is the number of non-consecutive subbands in NC-OFDM, and Q_j is the number of consecutive subcarriers of the jth subband. Therefore, the ith NC-OFDM symbol $\overline{x}_{i,j}(t)$ in the jth subband after N-Continuous technique is given by

$$\overline{x}_{i,j}(t) = \begin{cases} \sum_{k\in\mathbf{Q}_j} \overline{X}_{i,k}\, e^{j2\pi\frac{k}{T_s}t} & -T_{cp} \le t < T_s \\ 0 & elsewhere \end{cases} \quad (53)$$

where T_s is the symbol period, $\overline{X}_{i,k}$ is the updated data after N-Continuous technique, and $\mathbf{Q}_j = \{k_{j,1}, k_{j,2}, \ldots, k_{j,Q_j}\}$ is carrier set of the jth subband. Substituting (53) into (52) and rewriting it as an equivalent vector equation results

$$\mathbf{A}\boldsymbol{\Phi}\overline{\mathbf{x}}_i = \mathbf{A}\overline{\mathbf{x}}_{i-1} \quad (54)$$

where $\boldsymbol{\Phi} = diag(e^{j\psi k_{j,1}}, e^{j\psi k_{j,2}}, \ldots, e^{j\psi k_{j,Q_j}})$, $\psi = -2\pi\frac{Tcp}{Ts}$, $\overline{\mathbf{x}}_i = (\overline{X}_{i,k_{j,1}}, \overline{X}_{i,k_{j,2}}, \ldots, \overline{X}_{i,k_{j,Q_j}})^T$, and

$$\mathbf{A} = \begin{bmatrix} 1 & 1 & \cdots & 1 \\ k_{j,1} & k_{j,2} & \cdots & k_{j,Q_j} \\ \vdots & \vdots & & \vdots \\ k_{j,1}^{N'} & k_{j,2}^{N'} & \cdots & k_{j,Q_j}^{N'} \end{bmatrix}.$$

The suppression vector with minimum Euclidean-norm is found using the Moore-Penrose pseudo inverse of $\mathbf{A}\boldsymbol{\Phi}$ as equation

$$\mathbf{w}_i = -\mathbf{P}\,\mathbf{x}_i + \mathbf{P}\boldsymbol{\Phi}^H\overline{\mathbf{x}}_{i-1} \quad (55)$$

while $\mathbf{P} = \boldsymbol{\Phi}^H\mathbf{A}^H(\mathbf{A}\,\mathbf{A}^H)^{-1}\mathbf{A}\boldsymbol{\Phi}$, the updated signal vector [15] in the jth subband is given by

$$\overline{\mathbf{x}}_i = (\mathbf{I} - \mathbf{P})\mathbf{x}_i + \mathbf{P}\boldsymbol{\Phi}^H\overline{\mathbf{x}}_{i-1} \quad (56)$$

After the N-continuous technique the updated data $\overline{\mathbf{x}}_i$ is the input of SPC technique. SPC is an efficient PAPR reduction technique which reduces multiple peaks by a serial of weighted cancellation functions (WCF) [30].The frequency domain representation of SPC is derived with sampling interval T_s/K after N-continuous technique and is given by

$$\overline{x}_r = \frac{1}{\sqrt{k}}\sum_{k\in\mathbf{K}} \overline{X}_{i,k}\, e^{j2\pi\frac{k}{K}r} \quad (57)$$

where $\mathbf{K} = \mathbf{Q_1} \cup \mathbf{Q_2} \cup \ldots\ldots \cup \mathbf{Q_j}$ is the full band of the NC-OFDM spectrum. Assume that the amplitude of the wth sample is larger than the threshold TH, thus a cancellation function g_r which weighted by a factor α that is given by

$$\alpha = -\left(1 - \frac{TH}{|x_r|}\right)x \quad (58)$$

After the SPC the resultant signal $\tilde{x}_r$ [31] is

$$\tilde{x}_r = \overline{x}_r + \sum_{w\in\mathcal{W}} \alpha_w g_{r-w} \qquad |x_r| > TH \quad (59)$$

where $-N_s/2 + w + 1 < r \le N_s/2 + w$ with the truncated width N_s of WCF and wth sample $\in \mathcal{W}$ that is a sample index in NC-OFDM symbol. As a result of the band-limited characteristic of g_r, SPC do not seriously cause power leakage. After applying the Fourier transform to (59), it becomes

$$\tilde{X}_{i,k} = \overline{X}_{i,k} + d_{i,k} \quad (60)$$

which the cancellation variable $d_{i,k}$ and resultant signal after SPC $\tilde{X}_{i,k}$ is the Fourier transform of $\sum_{w\in\omega}\alpha_w g_{r-w}$ and $\tilde{x}_r$, respectively.

Based on (56) and (60), both of two techniques are adopted to signal processing in each subband of NC-OFDM parallelly. Therefore, the following analyses concentrate on the signal at the jth subband only and then it is extended to the whole band.

The power radiation in frequency domain is analyzed based on the above signal processing techniques. While $\mathbf{x}_i^{(v)}$ is the signal vector, $\mathbf{w}_i^{(v)}$ the suppression vector, and $\mathbf{d}_i^{(v)}$ is the cancellation vector where the "i" denotes the index of time slot and the (v) denotes the iteration number. In this subsection, the line that over a vector denotes the vector has been processed by N-Continuous scheme, for example, vector $\overline{\mathbf{x}}_i$ is the updated signal vector of vector $\mathbf{x}_i$ after N-Continuous process and $\tilde{\mathbf{x}}_i$ is the resultant signal vector of vector $\overline{\mathbf{x}}_i$ which is the input of IDFT.

In the first iteration, when the original signal is processed by N-Continuous method and SPC in sequence, the resultant signal vector is

$$\begin{aligned}\tilde{\mathbf{x}}_i^{(1)} &= \mathbf{x}_i + \mathbf{w}_i^{(1)} + \mathbf{d}_i^{(1)} \\ &= \mathbf{x}_i - \mathbf{P}\,\mathbf{x}_i + \mathbf{P}\boldsymbol{\Phi}^H\overline{\mathbf{x}}_{i-1} + \mathbf{d}_i^{(1)} \\ &= [(\mathbf{I}-\mathbf{P})\mathbf{x}_i + \mathbf{P}\boldsymbol{\Phi}^H\overline{\mathbf{x}}_{i-1}] + \mathbf{d}_i^{(1)} \qquad (61)\end{aligned}$$

After the second iteration, the resultant signal vector is

$$\begin{aligned}\tilde{\mathbf{x}}_i^{(2)} &= \tilde{\mathbf{x}}_i^{(1)} + \mathbf{w}_i^{(2)} \\ &= (\mathbf{I}-\mathbf{P})\mathbf{x}_i + (\mathbf{I}-\mathbf{P})\mathbf{d}_i^{(1)} + \mathbf{P}\boldsymbol{\Phi}^H\overline{\mathbf{x}}_{i-1} - \mathbf{P}\boldsymbol{\Phi}^H\mathbf{P}\overline{\mathbf{x}}_{i-1} \\ &\quad + \mathbf{P}\boldsymbol{\Phi}^H\mathbf{P}\boldsymbol{\Phi}^H\overline{\overline{\mathbf{x}}}_{i-2} + \mathbf{P}\boldsymbol{\Phi}^H\overline{\mathbf{d}}_{i-1}^{(1)} + \mathbf{d}_i^{(2)} \\ &= [(\mathbf{I}-\mathbf{P})\mathbf{x}_i + \mathbf{P}\boldsymbol{\Phi}^H\overline{\mathbf{x}}_{i-1}] + \mathbf{P}\boldsymbol{\Phi}^H\mathbf{P}\boldsymbol{\Phi}^H\overline{\overline{\mathbf{x}}}_{i-2} \\ &\quad + [(\mathbf{I}-\mathbf{P})\mathbf{d}_i^{(1)} + \mathbf{P}\boldsymbol{\Phi}^H\overline{\mathbf{d}}_{i-1}^{(1)}] \\ &\quad - \mathbf{P}\boldsymbol{\Phi}^H\mathbf{P}\overline{\mathbf{x}}_{i-1} + \mathbf{d}_i^{(2)} \\ &= [(\mathbf{I}-\mathbf{P})\mathbf{x}_i + \mathbf{P}\boldsymbol{\Phi}^H\overline{\mathbf{x}}_{i-1}] + [(\mathbf{I}-\mathbf{P})\mathbf{d}_i^{(1)} + \mathbf{P}\boldsymbol{\Phi}^H\overline{\mathbf{d}}_{i-1}^{(1)}] \\ &\quad + \mathbf{P}\boldsymbol{\Phi}^H\mathbf{P}\boldsymbol{\Phi}^H\mathbf{w}_{i-2}^{(2)} \\ &\quad + \mathbf{d}_i^{(2)} \qquad (62)\end{aligned}$$

Comparing the $\tilde{\mathbf{x}}_i^{(1)}$ with $\tilde{\mathbf{x}}_i^{(2)}$, the cancellation vector $\mathbf{d}_i^{(1)}$ is processed by N-continuous technique to further suppress its sidelobes, while the noise term $(\mathbf{P}\boldsymbol{\Phi}^H\mathbf{P}\boldsymbol{\Phi}^H\mathbf{w}_{i-2}^{(2)})$ and $\mathbf{d}_i^{(2)}$ have lower sidelobe power than $\mathbf{d}_i^{(1)}$ because the sidelobe power of $\tilde{\mathbf{x}}_i^{(1)}$ is lower than the original $\mathbf{x}_i$. Therefore the sidelobe of $\mathbf{x}_i^{(2)}$ is lower than that of $\mathbf{x}_i^{(1)}$.

Since N-Continuous technique does not change the original PAPR [16], therefore the first two terms in (61) do not change the original PAPR. From (59), The PAPR of the signal after SPC satisfies:-

$$\frac{\max\limits_{r}\{|\tilde{x}_r|^2\}}{E\{|\tilde{x}_r|^2\}} < \frac{\max\limits_{r}\{|x_r|^2\}}{E\{|x_r|^2\}} \qquad (63)$$

The cancellation vector is generated with the knowledge of the suppression vector which the affection of sidelobe suppression to PAPR reduction can be reduced during the further processing. Therefore, both the values of cancellation vector and suppression vector reduce with the repeated processing. Furthermore the interaction of them is degraded iteratively and the PAPR performance is improved. This cancellation vector has relatively low impact on the power spectrum. Therefore this technique improves both PAPR reduction and sidelobe suppression.

G- Advanced Cancelation Carrier with Signal Set Expansion

This technique is a combination between two techniques SSE and ACC that reduce the PAPR and sidelobe power, respectively which are added after S/P converter as shown in Fig. 10. While the sequence after SSE has low PAPR, P cancellation carriers (CC) are inserted in the left and right hand side of this sequence to reduce the sidelobe power. These CCs are not used for data transmission, but it carry weighting factors $w_p, p = 1, \ldots\ldots P$, which can determined such that reduce the sidelobe power.

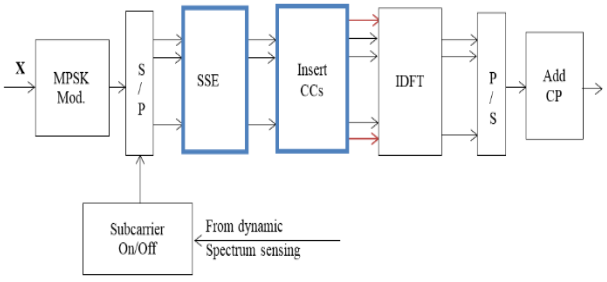

Figure 10. Block diagram of a NC-OFDM transmitter with adding SSE and ACC techniques [17].

1) SSE for PAPR reduction:

The key idea of SSE is to exploit the expanded signal from the original signal to reduce the PAPR. The symbols of a modulation technique which modulates d bits/symbol and consists of 2^d points, are mapped to another modulation technique which modulates $(d+a)$ bits/symbol and consists of 2^{d+a} points. Therefore each point in the original symbol is associated with $2^{d+a}/2^d$ points in the expanded symbol. The basic idea is computing the PAPR for the different combinations and the sequence with minimum PAPR is chosen for transmission. The points of the expanded signal set that associated with the points in the original signal is assumed to be known in the transmitter and receiver therefore, no side information are needed at the receiver to demodulate the transmitted data. For example, mapping QPSK to 8-PSK is shown in Fig. 11, each subcarrier in QPSK can take either $\mathrm{a}, \mathrm{b}, \mathrm{c}, \mathrm{d}$ (data symbol) while point a is associated with $\mathrm{a}_1, \mathrm{a}_2$ in 8-PSK and also the rest of points. The phase difference between two points in the expanded signal that are associated to one point in the original signal is φ, that can be $\pi/4$, $3\pi/4$, $5\pi/4$, and $7\pi/4$.

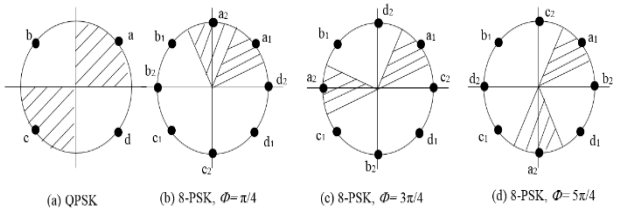

Figure 11. Mapping the symbols from QPSK to 8-PSK [19].

This mapping may be done by many ways that differ in computational complexity. Mapping all symbols of original signal to their associated points at once achieves large reduction but the complexity is increased. This method is practically not realizable because of its high complexity. Therefore another simple mapping method is used that is based on changing the first symbol among all associated points one by one and computing the PAPR for each case and the signal point that achieves the lowest PAPR is chosen for transmission. Then these steps are repeated in the same way for all X_k. Assume $X_k \in (\mathrm{a}, \mathrm{b}, \mathrm{c}, \mathrm{d})$ and each symbol of $X_k$is mapped to one of associated points X_{k1} *or* X_{k2} while X_k will be modified to X'_k and forming $\mathrm{X}' = (X'_0, X'_1, \ldots\ldots, X'_K)$

$$X'_k = \arg\min_{X_n} \mathrm{PAPR\ for}\ [X_k] \tag{64}$$

There is another method that used for this mapping which have low complexity and called data block mapping method. It depends on dividing the symbol X into s_b sub-blocks while each sub-block contains K/s_bcarriers. This changes the symbols block by block instead of one by one as mentioned while it reduces the complexity but do not reduce the PAPR efficiently as simple mapping method.

At the receiver, the signal points that lay around $\mathrm{a}_1 \mathrm{or}\, \mathrm{a}_2$ is converted to a point which has minimum Euclidean distance from each received symbol therefore, side information is not needed in this technique. While X'_n with minimum PAPR is achieved from X_n input data by applying SSE technique but the high sidelobe power constrains is still exist and it should be illuminated.

2) ACC Technique:-

After applying the SSE technique, ACC technique is used for reducing the sidelobe power. This technique based on adding P cancellation carriers to K subcarriers to achieve this reduction. After reducing the PAPR, X′ is used to compute the spectrum and the sidelobe power. The spectrum of each individual subcarrier is computed as:-

$$\mathcal{S}_k(F) = X'_k \,.\frac{\sin\big(\pi(F - F_k)\big)}{\pi(F - F_k)},$$
$$k = 0, \ldots\ldots, K-1 \tag{65}$$

where F is normalized frequency shifted to the center frequency as (8), F_k is normalized center frequency of kth subcarrier. The spectrum of OFDM symbol is given by,

$$\mathcal{S}(F) = \sum_{k=0}^{K-1} \mathcal{S}_k(F) \tag{66}$$

The average sidelobe power equation over N samples is given by [22],

$$\Lambda = \frac{1}{N}\sum_{n=1}^{N}\left|\sum_{k=0}^{K-1} X'_k \,.\frac{\sin(\pi(F'_n - F_k))}{\pi(F'_n - F_k)}\right|^2 \tag{67}$$

where, F'_n is the normalized frequency sample at nth sample.

The cancellation carrier technique operates with inserting carriers with optimized weights in the left and right hand side of the OFDM spectrum while these carriers do not carry any information. The objective is calculating this optimized weight to cancel out the sidelobes of the original signal.

ACC technique depends on inserting P carriers in the left and right hand side of the OFDM spectrum. The spectrum of pth cancellation carrier is expressed as,

$$C_p(F) = \frac{\sin\left(\pi\big(F - F_p\big)\right)}{\pi\big(F - F_p\big)}, \tag{68}$$

where $p = 1, \ldots\ldots P$, F_p is normalized center frequency of the pth CC. These carriers are multiplied by $w_p, p = 1, \ldots\ldots P$ weighting factor which is calculated such that the minimum average sidelobe power is achieved to reduce the sidelobes in the OFDM spectrum. The total spectrum of OFDM symbol with inserting P CC is expressed as,

$$\mathcal{S}_T(F) = \mathcal{S}(F) + \sum_{p=1}^{P} w_p . C_p(F) \tag{69}$$

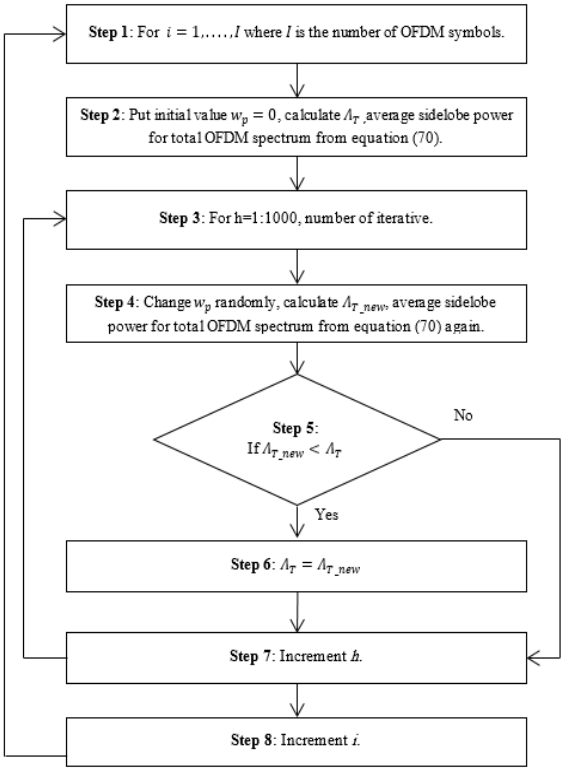

Figure 12. Flow chart of the technique used for choosing the minimum sidelobe power [17].

The average sidelobe power over N samples for total spectrum of OFDM symbol is given by,

$$\Lambda_T = \frac{1}{N}\sum_{n=1}^{N} |\mathcal{S}_T(F_n')|^2. \qquad (70)$$

Computing of weighting factors is based on iterative process to find the optimal weight. This optimization weight w_p is a complex values that lies between 0, 1. In the first $w_p = 0$ is put as initial values while the total OFDM spectrum $\mathcal{S}_T(F)$ and the average sidelobe power Λ_T are computed. It is noted that, it is equal to the original spectrum without adding CCs. After that w_p is changed randomly under the range from 0 to 1 and the total OFDM spectrum and the average sidelobe power are computed again. This process is repeated iteratively as shown in Fig. 12 until the minimum average sidelobe power is obtained. At that power the optimum weighting factors are obtained for each cancellation carrier.

4. SIMULATION RESULTS

NC-OFDM signal with random distributions of 64 subcarriers are used in our simulation. This simulation focuses on comparing the all techniques and testing the effectiveness of them on sidelobe suppression, PAPR reduction, bit error rate (BER) and system complexity. The details of the Implementation parameters of these techniques are included in Table 1 [8]-[11], [14], [15], [17].

TABLE 1: IMPLEMENTATION PARAMETERS OF THE PROPOSED TECHNIQUE.

Parameter	Value
Number of iteration	1000
Number of subcarriers$K$	64
T_{cp}/T_0	1/8
Modulation scheme	QPSK
No. of alternative sequences in MCS C	4
No. of choice sequences in SLM D	3
No. of interleavers M	4
Expanded modulation scheme	8-PSK
Number of subcarrier that used for expansion L	$K/8$
Phase difference φ	$3\pi/4$
Redundancy$R$	3
Length of cyclic prefix η	8
No. of distinct and consecutive block V	2
Number of subblocks in the first and last blocks $\mathcal{N}$	8
The derivative N'	0
Number of iterations in NC-SPC "$iter$"	1
Number of quantized phase shift	4
Number of added cancellation carriers$P$	4
noise	AWGN

The average sidelobe power is computed over 1000 random input symbol that modulated with QPSK. For SLM-MCS technique 4 alternative sequences are used and 3 sequences with minimum sidelobe power are chosen. When adding interleaver to the previous technique that becomes I-SLM-MCS, 4 interleavers are used. In ACEPR technique $K/8$ subcarriers are used for expansion with phase shift $3\pi/4$ and the rest of subcarrier are partitioned to reduce PAPR. The hybrid precoding technique with redundancy $R = 3$ are also shown while this value should be decided adaptively due to the system's requirement and wireless condition. Four quantized phase shift, $V = 2$, and $\mathcal{N} = 8$ are considered in MS-PTS technique. With the NC-SPC technique, the note "$iter$" denotes the number of iterations and $N' = 0$ is used. For ACC-SSE technique

4 CCs are added in the left and right hand side of the OFDM symbol (2CCs in each side) and the phase difference is 3pi/4. While changing any parameters from the previous parameters, leads to change the corresponding sidelobe power and PAPR. All the simulation results have been carried out using a computer platform with the following specification (2.13 GHZ processor, 4GB RAM, and 512 GB hard disk)

Fig. 13, shows the effect of sidelobe power for all techniques that should be decreased. The normalized power spectrum of these techniques is compared with the original NC-OFDM. The figure shows that the sidelobe power is reduced by about 9, 12, 15, 21.5, 24, 25, and 34 dB for SLM-MCS, ACEPR, I-SLM-MCS, hybrid precoding, MS-PTS, NC-SPC, and ACC-SSE, respectively at the $K/4$ subcarrier distance from the band-edge compared to the original NC-OFDM. The PSD is shown in another representation for more illustration which is shown in Fig. 14.

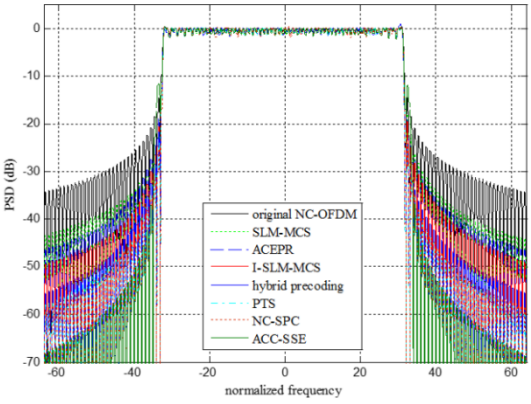

(a)

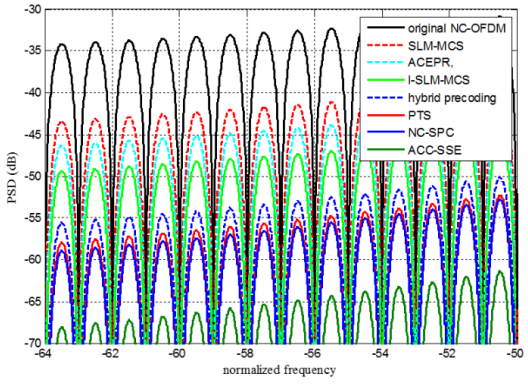

(b)

Figure 13. The power spectral density for all techniques compared with original NC-OFDM technique, (a) the main figure, (b) its zoom.

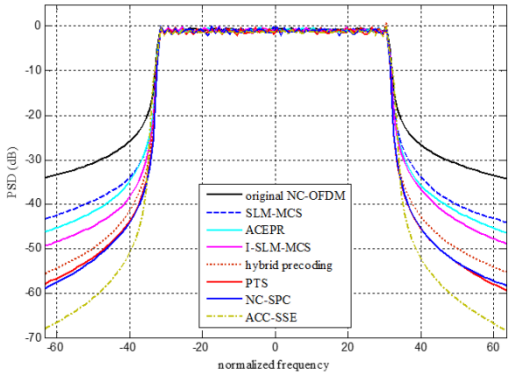

Figure 14. Another representation for the PSD of all techniques with original technique.

The performance of the all techniques is presented in terms of the Complementary Cumulative Distribution Function (CCDF). The CCDF is the probability of exceeding the PAPR of an NC-OFDM signal over a given threshold PAPRth and is expressed as,

$$\mathrm{CCDF}\left(\mathrm{PAPR}(x(\mathrm{t}))\right) = \Pr\left(\mathrm{PAPR}(x(\mathrm{t})) > \mathrm{PAPR}_{Th}\right) \quad (71)$$

The performance of the original NC-OFDM technique and the other techniques for 64 subcarrier in terms of CCDF is shown in Fig. 15. The PAPR reduction at CCDF = 10-3 is about 1.7, 2.4, 2.4, 3.45, 4.6, 5.25, and 5.25dB for MS-PTS, SLM-MCS, ACEPR, I-SLM-MCS, ACC-SSE, NC-SPC, and hybrid precoding techniques, respectively compared to the original NC-OFDM.

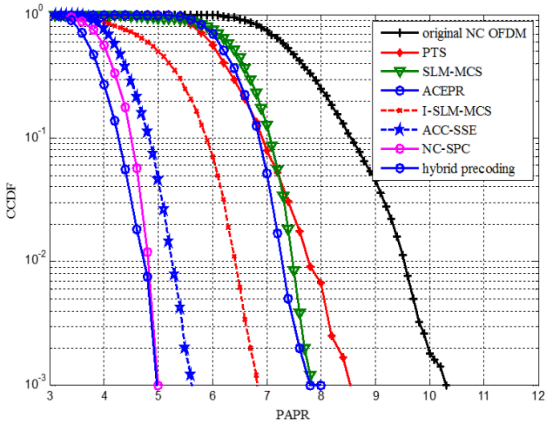

Figure 15. CCDF of PAPR for all techniques and original NC-OFDM technique.

The performance of the signal to noise ratio (SNR) with bit error rate (BER) under Additive White Gaussian Noise (AWGN) channel for original NC-OFDM and all other techniques is shown in Fig. 16. The reduction of joint PAPR and sidelobe power affects

on the BER performance. However, for fair comparison, let us consider a NC-OFDM system with adjacent channel interference constraint. At BER=10^{-2} the SNR is 13.2, 11.1, 10.3, 10.2, 8.2, 8.2, 7.3, and 7.25 dB for ACC-SSE, ACEPR, MS-PTS, NC-SPC, original NC-OFDM, hybrid precoding, SLM-MCS, and I-SLM-MCS, respectively. From this figure, we can conclude that some techniques improve the BER performance such as SLM-MCS and I-SLM-MCS techniques while the hybrid precoding technique do not change the performance and the rest of the techniques degrade the BER performance.

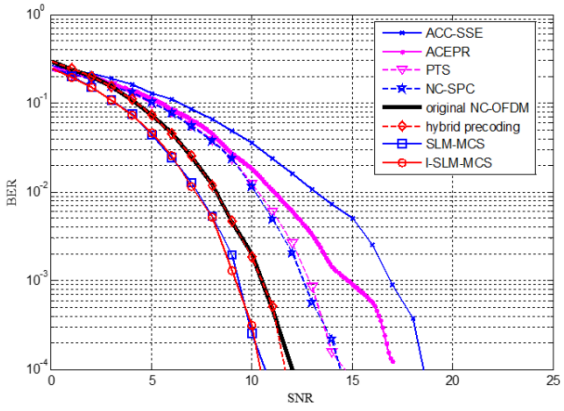

Figure 16. BER Vs SNR for all techniques and original NC-OFDM technique.

Table 2, presents a comparative study between the simulation results of the different techniques for the case $K = 64$. In this table the sidelobe power is computed at the $K/4$ subcarrier distance from the band-edge. The PAPR and SNR are also computed at CCDF=10-3 and BER=10-2, respectively. The`CPU time and system complexity are investigated and compared with original NC-OFDM.

TABLE 2: COMPARATIVE STUDY BETWEEN THE SIMULATION RESULTS OF THE DIFFERENT TECHNIQUES FOR $\boldsymbol{K = 64}$.

	Original NC-OFDM	SLM-MCS	ACEPR	I-SLM-MCS	Hybrid Pre-coding	MS-PTS	NC-SPC	ACC-SSE
Sidelobe power at $F = -64$	-34 dB	-43 dB	-46 dB	-49 dB	-55.5 dB	-58 dB	-59 dB	-68 dB
PAPR at CCDF=10^{-3}	10.25 dB	7.85 dB	7.85 dB	6.8 dB	5 dB	8.55 dB	5 dB	5.65 dB
SNR at BER=10^{-2}	8.2 dB	7.3 dB	11.1 dB	7.25	8.2 dB	10.3 dB	10.2 dB	13.2 dB
CPU time(in minutes)	3.45 min.	9.32 min.	11.52 min.	16.43 min.	8.20 min	22.15 min.	12.14 min.	20.25 min.
Relative Complexity	low	medium	medium	high	medium	high	medium	high

It is noted that, the ACC-SSE technique has the minimum sidelobe power and the lower PAPR but also has the maximum SNR. This means that it improves the sidelobe power and PAPR but also reduces the BER performance and have high complexity. On the other side, the SLM-MCS technique improves the BER performance (reduces the SNR) with medium complexity but with low reduction for the sidelobe power and PAPR. I-SLM-MCS improves the sidelobe power, PAPR, and BER performance than SLM-MCS but increases the complexity. Therefore, it is evident that no approach can be considered as optimum for all the performance measured metrics.

5. CONCLUSIONS

In this paper, we present the different techniques that reduce joint sidelobe power and PAPR in OFDM based cognitive radio and compare between them. The comparative study between the different techniques has been covered out based on sidelobe power, PAPR, BER, and complexity. The hybrid precoding technique is considered the optimum one for all techniques.

References:

[1] R. Rajbanshi, A. M. Wyglinski, and G. J. Minden, "An efficient implementation of NC-OFDM transceivers for cognitive radios," *1st Int. Conf. on CROWNCOM, Mykonos Island, Greece*, pp. 1-5, Jun. 2006.

[2] Federal Communications Commission, "*Spectrum policy task force*," Rep., ET Docket no. 02-135, November 2002.

[3] S. Kumar, J. Sahay, G. K. Mishra, and S. Kumar, "Cognitive radio concept and challenges in dynamic spectrum access for the future generation wireless communication systems," *Wireless Personal Communications*, vol. 59, no. 3, pp. 525–535, 2011.

[4] J. Mitola, "*Cognitive radio: an integrated agent architecture for software defined radio*," *Tekn. Dr. dissertation, Royal Inst. Tech. (KTH)*, Stockholm, Sweden, 2000.

[5] H. Sakran, M. Shokair, S. El-Rabaie, and O. Nasr, "Study the effect of PAPR on wideband cognitive OFDM radio networks," *Telecommunications Systems*, vol. 53, pp. 469-478, 2013.

[6] H. Sakran, M. Shokair, and A. A. Elazm, "An efficient technique for reducing PAPR of OFDM system in the presence of nonlinear high power amplifier," *Progress In Electromagnetics Research C*, vol. 2, pp. 233–241, 2008.

[7] H. Sakran, O. Nasr, and M. Shokair, "An efficient adaptive technique with low complexity for reducing PAPR in OFDM-based Cognitive Radio," *ISRN Signal Processing*, Article ID 584941, http://dx.doi.org/10.5402 /2012/ 584941, 7 pages 2012.

[8] A. Ghassemi, L. Lampe, A. Attar, and T. Gulliver, "Joint sidelobe and peak power reduction in OFDM-Based cognitive radio," *in proceeding IEEE, 72nd Vehicle Technology Conference*, pp. 1-5, sept. 2010.

[9] A. Selim, B. Ozgul, and L. Doyle, "Efficient sidelobe suppression for OFDM systems with peak-to-average power ratio reduction," *IEEE International Symposium on Dynamic Spectrum Access Network*, pp. 510–516, 2012.

[10] A. Rady, M. Shokair, S. El-Rabaie, and A. El-Korany, "Two proposed approaches for minimization of both sidelobe and PAPR in cognitive radio network," *in proceeding IEEE, 31st national radio science conference (NRSC)*, pp. 124-131, 2014.

[11] A. Rady, M. Shokair, S. El-Rabaie, and A. El-Korany, "A hybrid precoding technique for reducing both PAPR and sidelobe power in cognitive radio networks", *Circuits and Systems: An International Journal (CSIJ)*,vol. 1, no. 3, pp. 67-76, July 2014.

[12] J. Baig, and V. Jeoti, "PAPR reduction in ofdm systems: zadoff-chu matrix transform based pre/post-coding techniques." *in proceeding IEEE, Computational Intelligence, Communication Systems and Networks (CICSyN)*, pp. 373 – 377, july 2010.

[13] J. Mountassir, A. Isar, and T. Mountassir, "Precoding techniques in OFDM systems for PAPR minimization," *In proceeding of: IEEE MELECON*, 2012.

[14] A. Tom and H. Arslan, "Joint sidelobe suppression and PAPR reduction in OFDM using partial transmit sequences", *in proceeding of IEEE military communication conference*, pp. 95-100, 2013.

[15] P. Wei, L. Dan, J. Wang, Y. Xiao, Xu He and S. Li , "Performance analysize of joint processing of sidelobe suppression and PAPR reduction in NC-OFDM systems", *in proceeding of IEEE International ICST Conference on Communications and Networking (CHINACOM)*, pp. 108-113, 2011.

[16] J. van de Beek and F. Berggren, "N-continuous OFDM," *IEEE Communication Letter*, vol. 13, no. 1, pp. 1 –3, Jan. 2009.

[17] A. Rady, M. Shokair, S. El-Rabaie, and A. El-Korany, "Efficient Technique for Sidelobe Suppression and PAPR Reduction in OFDM-Based Cognitive Radios",*Wireless Pers Commun*, DOI: 10.1007/s11277-015-2390-6, Mar. 2015.

[18] S. Brandes, I. Cosovic, and M. Schnell, "Sidelobe suppression in OFDM systems by insertion of cancellation carriers", *in proceeding IEEE Vehicle Technology Conference*, vol. 1, pp. 152-156, 2005.

[19] S. H. Han, and J. H. Lee, "Peak-to-average power ratio reduction of an OFDM signal by signal set expansion", *IEEE International Conference Communication*, vol. 2, pp. 867-871, 2004.

[20] I. Cosovic, and T. Mazzoni, "Suppression of sidelobes in OFDM systems by multiple-choice sequences," *European Trans. Telecommun.*, vol. 17, no. 6, pp. 623–630, June 2006.

[21] L. Xin, W. Qihui, and Y. Yang, "A new SLM OFDM scheme with low complexity for PAPR reduction in CR system," *in Proceeding IEEE International Conference on Wireless Information Technology and Systems (ICWITS '10)*, pp. 1–4, September 2010.

[22] I. Cosovic, and V. Janardhanam, "Sidelobe suppression in OFDM systems," *in Proceeding of International Workshop on Multi-Carrier Spread-Spectrum (MC-SS'05)*, pp. 473-482, September 2005.

[23] S. Pagadarai, R. Rajbanshi, A. M. Wyglinski, and G. J. Minden, "Sidelobe suppression for OFDM-based cognitive radios using constellation expansion," *in proceeding of IEE Wireless Communications and Networking Conference, WCNC*, pp. 888-893, 2008.

[24] Z. Yuping, "In-band and out-band spectrum analysis of OFDM communication systems using ICI cancellation methods," *in Proceedings of International Conference on Communication Technology. 'WCC – ICCT*, vol.1, pp. 773-776, 2000.

[25] A. Ghassemi and T. A. Gulliver, "a low-complexity PTS-based radix FFT method for PAPR reduction in OFDM systems," *Signal Processing, IEEE Transactions on*, vol. 56, pp. 1161-1166, 2008.

[26] A. Tom, A. Sahin, and H. Arslan, "Mask compliant precoder for OFDM spectrum shaping," *IEEE Communication Lett*er, vol. 17, no. 3, pp. 447–450, 2013.

[27] Z.-Q. Luo, W.-K. Ma, A.-C. So, Y. Ye, and S. Zhang, "Semidefinite relaxation of quadratic optimization problems," *IEEE Signal Processing Magazine*, vol. 27, no. 3, pp. 20–34, 2010.

[28] S. H. Muller and J. B. Huber, "OFDM with reduced peak-to-average power ratio by optimum combination of partial transmit sequences," *Electron. Lett.*, vol. 33, no. 5, pp. 368–369, Feb. 997.

[29] Y. Zhou, A. M. Wyglinski, "On sidelobe suppression for multicarrier- based transmission in dynamic spectrum access networks," *IEEE Transaction on Vehicle Technology*, vol. 59, no. 4, pp. 1998-2006, May 2010.

[30] L. L. Dan, Y. Xiao, W. Ni, S. Q. Li, "Improved peak cancellation for PAPR reduction in OFDM systems," *IEICE Transaction on Commun*ication, vol. E93. B, Issue 1, pp. 198-202, 2010.

[31] G. G. Chen, R. Ansari, Y. W. Yao, "Improved peak windowing for PAPR reduction in OFDM," *IEEE 69th VTC Spring*, pp.1-5, Apr. 2009.

Asmaa Rady received her B.Sc. degree in electronics and electrical communications engineering from the Faculty of Electronic Engineering, Menoufia University, Egypt, in 2009. Currently, she is working towards her M.Sc. degree at the Faculty of Electronic Engineering, Menoufia University, Egypt. Her current research areas of interest include cognitive radio networks and joint peak to average power ratio reduction and sidelobe suppression in cognitive radio networks.

El-Sayed El-Rabaie (Senior Member, IEEE' 1992-MIEE Chartered Electrical Engineer). He Received the B.Sc. Degree with Honors in Radio Communications from Tanta University, EGYPT, 1976, the M.Sc. Degree in Communication Systems From Menoufia University, EGYPT, 1981, and the Ph.D. Degree in Microwave Device Engineering From the Queen's University of BELFAST, 1986. He was a Postdoctoral Fellow at Queen's (Dept. of Electronic Eng.) up to Feb. 89. He has shared in Translating the First Part of the

Arabic Encyclopedia. Now he is Involved in Different Research Areas, Member of the National Electronic and Communication Eng. Promotion, and Reviewer of Quality Assurance and Accreditation of Egyptian Higher Education.

Mona Shokair received the B.E. and M.E. degrees in electronics engineering from El Menoufia University, El-Menoufia, Egypt, in 1993 and 1997, respectively. She received Ph.D. from Kyushu University, Japan, 2005. Since 2005, she is lecturer in El-Menoufia University. She received VTS chapter IEEE award from Japan in 2003. Now she is working in OFDM system, WIMAX system and cognitive radios.

Ahmed S. Elkorany received the B.Sc. degree in electronics and electrical communications (with honor degree) in May 2003 from faculty of electronic engineering, Menoufia University. He is appointed as a Demonstrator in Dec. 2003. In the same dept. He received the M.Sc. and the Ph.D. in electrical communications (microwaves and antennas) in 2007 and 2011, respectively, both from the same faculty. Finally in Dec. 2011 he was appointed as a Lecturer also in the same dept. His research is focused on, numerical techniques, CAD tools, programming languages, UWB antennas and systems, EBG structures and cognitive radio.